2023 62nd IEEE Conference on Decision and Control (CDC)
December 13-15, 2023. Marina Bay Sands, Singapore

Spectral Decomposition in Kalman Filter Algorithm for Homogeneous Atomic Clock Ensembles

Yuyue Yan, Takahiro Kawaguchi, Yuichiro Yano, Yuko Hanado, and Takayuki Ishizaki

Abstract— **Existing studies have pointed out numerical instability in the Kalman filter of atomic clocks, but the reasons for such instability have not been clarified mathematically. In this paper, we mathematically clarify the reason for the numerical instability by a new approach of spectral decomposition of the error covariance matrix in the Kalman filter. In particular, we reveal the fact that the error covariance matrix for homogeneous undetectable atomic clock ensembles can be decomposed into a diverging part and a converging part. Furthermore, the Kalman gain is solely influenced by the converging part, but not the diverging part, meaning that the Kalman gain converges to a steady-state value if ideal computation is possible without computation error. We present an alternative method to the conventional Kalman filter to avoid numerical instability and reduce computation cost where the covariance of Kalman filter can be computed rigorously only using three n-dimensional Riccati iterations instead of an nN-dimensional Riccati iterations for an n-order clock model with N clocks. A numerical example is provided to illustrate the efficacy of our approach.**

I. Introduction

Atomic clocks are fundamental devices to generate accurate time scales for many fields in our daily life. Many applications in which the technologies directly or indirectly depend on time scales benefited from the development of atomic clocks (see [1] and the references therein). For example, the atomic clocks onboard the satellites and on the earth stations play an essential role to achieve user positioning by Global Positioning Systems. To improve the accuracy of the atomic clocks for the development of modern technologies, the researchers in the time and frequency community obtained experimental evidence and reliable models for the atomic clocks. Since it is revealed experimentally that the time deviation of atomic clocks can be characterized as a random noise (so-called, clock noise), the time deviations are properly modeled by the stochastic processes under stochastic differential equations.

In order to keep precise and reliable time, an ensemble of atomic clocks are used by the national metrology institutes (NMIs) in many countries to generate their national time scales. In such a time generation process, how to properly deal with the prediction problem for the phase noises is the main problem to ensure excellent performance. As an effective method for predicting noises in the fields of signal processing, the Kalman filter has been implemented in time scale generation for estimating the difference between two clocks [2]–[5]. However, practical implementations often ignore the fact that the system of the atomic clock ensemble is undetectable due to its inherent properties in measurements, even though detectability is considered as a necessary condition for constructing a Kalman filter as an optimal prediction algorithm [6], [7]. Since the detectability condition is broken, the entries of the error covariance matrix of the Kalman filter grow unboundedly due to computational errors, which may lead to non-negligible numerical instability [8].

To deal with the problem, Brown proposed a covariance reduction method to keep the error covariance matrix from running away [9]. Greenhall developed a reduction method that works well in the presence of noisy measurements using some weighting parameters solved from an 1-parameter least-squares problem [4], [10]. The key to both approaches is how to modify the error covariance matrix of the Kalman filter and suppress its divergence. The performance of both methods depends on the value of initial error covariance matrix in the Kalman filter.

In the literature, the prediction problem for undetectable systems is not the main focus in the systems and control field because we may be able to reset the sensors to re-design the measurement policy in the practice to make a re-designed control system detectable. However, in the atomic clock ensembles, the sensors are impossible to make it detectable due to a physical restriction.

In this paper, we focus on how to theoretically understand the essential reason why numerical instability happens in the Kalman filter for homogeneous atomic clock ensembles. To this end, we apply spectral decomposition to atomic clock ensembles decomposing the error covariance matrix of the Kalman filter into several parts. The main contributions are summarized as follows.

1) We reveal the fact that the error covariance matrix of the conventional Kalman filter for homogeneous undetectable atomic clock ensembles can be decomposed into a diverging part and a converging part. It is found that the Kalman gain is solely influenced by the converging part but not the diverging part, meaning that the Kalman gain converges to a steady-state value if ideal computation without computation error is possible.
2) Based on spectral decomposition, we present an alternative Kalman filtering method to avoid numerical instability and reduce computation cost where the co-

Yuyue Yan and Takayuki Ishizaki are with the Department of Systems and Control Engineering, Tokyo Institute of Technology, Meguro, Tokyo 152-8552 Japan (e-mail: yan.y.ac@m.titech.ac.jp, ishizaki@sc.e.titech.ac.jp). Takahiro Kawaguchi is with the Division of Electronics and Informatics, Gunma University, Kiryu, Gunma 371-8510 Japan (e-mail: kawaguchi@gunma-u.ac.jp). Yuichiro Yano and Yuko Hanado are with the National Institute of Information and Communications Technology, Koganei, Tokyo 184-0015 Japan (e-mail: y-yano@nict.go.jp, yuko@nict.go.jp).

variance of Kalman filter can be computed rigorously only using three n-dimensional Riccati iterations instead of an nN-dimensional Riccati iterations for an n-order clock model with N clocks.

Notation We write $\mathbb{R}$ for the set of real numbers, $\mathbb{R}_+$ for the set of positive real numbers, $\mathbb{R}^n$ for the set of n-dimensional real column vectors, $\mathbb{N}_+$ for the set of positive integers, and $\mathbb{R}^{n\times m}$ for the set of n by m real matrices. Moreover, $\otimes$ denotes Kronecker product, $(\cdot)^\mathsf{T}$ denotes the transpose, $(\cdot)^\dagger$ denotes the Moore-Penrose pseudoinverse, $\mathsf{diag}(\cdot)$ denotes a diagonal matrix, $\mathbb{1}_n$ denotes the n-dimensional all-ones vector, and I_n denotes the n-dimensional identity matrix.

II. Mathematical Model

A. Single Clock in Homogeneous Clock Ensemble

Consider a discrete-time sequence $\{t_0, t_1, \dots, t_T\}$ in an ideal time scale, where the interval between two adjacent times is assumed to be a constant sampling period τ, i.e.,

$$t_k := \tau k, \quad k = 0, 1, \dots, T. \tag{1}$$

Let $n \in \mathbb{N}_+$ denote the order of an atomic clock model, which is assumed to be identical for all clocks labeled by $j \in \mathcal{N} := \{1, 2, \dots, N\}$ in the ensemble. Then, the stochastic processes of the phase deviation [11] of each clock $j \in \mathcal{N}$ in the clock ensemble can be represented by the discrete-time linear stochastic system

$$\Sigma^j : \begin{cases} x^j[k+1] = Ax^j[k] + v^j[k] \\ \Delta h^j[k] = Cx^j[k] \end{cases} \tag{2}$$

where $x^j = [x_1^j, \dots, x_n^j]^\mathsf{T} \in \mathbb{R}^n$ denotes the state vector, $\Delta h^j[k] \in \mathbb{R}$ denotes the time deviation, $v^j = [v_1^j, \dots, v_n^j]^\mathsf{T} \in \mathbb{R}^n$ denotes the noise vector, and the matrices A and C are defined as

$$A := A_\tau := \begin{bmatrix} 1 & \tau & \frac{\tau^2}{2} & \cdots & \frac{\tau^{n-1}}{(n-1)!} \\ 0 & 1 & \tau & \cdots & \frac{\tau^{n-2}}{(n-2)!} \\ \vdots & & \ddots & \ddots & \vdots \\ \vdots & & & 1 & \tau \\ 0 & 0 & \cdots & \cdots & 1 \end{bmatrix} \tag{3}$$

$$C := \begin{bmatrix} 1 & 0 & \cdots & 0 \end{bmatrix}. \tag{4}$$

The noise $v^j[k]$ is a white Gaussian process such that

$$\mathbb{E}\big[v^j[k]\big] = 0, \quad \mathbb{E}\big[v^j[k]{v^j}^\mathsf{T}[k]\big] = Q,$$

where the covariance matrix is given as

$$Q := \int_0^\tau A_t \mathsf{diag}(q_1, \dots, q_n) A_t^\mathsf{T} dt \tag{5}$$

for some nonnegative values $q_i \geq 0$, $i = 1, \dots, n$. Note that A_t in (5) is understood as A_τ with τ replaced by t [12]. The detailed physical background of the model can be found in [13] and the references therein.

B. Atomic Clock Ensemble With Measurement

For the presentation below, we let the discrete-time state $\boldsymbol{x}$ of the overall clocks be defined as

$$\boldsymbol{x} := \begin{bmatrix} \boldsymbol{x}_1 \\ \vdots \\ \boldsymbol{x}_n \end{bmatrix} \in \mathbb{R}^{nN}, \quad \boldsymbol{x}_i := \begin{bmatrix} x_i^1 \\ \vdots \\ x_i^N \end{bmatrix} \in \mathbb{R}^N,$$

and the system noise $\boldsymbol{v}$ as

$$\boldsymbol{v} := \begin{bmatrix} \boldsymbol{v}_1 \\ \vdots \\ \boldsymbol{v}_n \end{bmatrix} \in \mathbb{R}^{nN}, \quad \boldsymbol{v}_i := \begin{bmatrix} v_i^1 \\ \vdots \\ v_i^N \end{bmatrix} \in \mathbb{R}^N.$$

In terms of the physical meaning, note that the variables $\boldsymbol{x}_1$, $\boldsymbol{x}_2$, and $\boldsymbol{x}_3$ represent the vector of phase deviations, random walk components, frequency drifts of all the overall clocks [3], respectively, and the remaining other variables represent some components in higher-dimensional cases.

As a measurement output, the difference between the phase deviations of clocks i and j, i.e., $\Delta h^i[k] - \Delta h^j[k]$, is only measurable due to physical restrictions. Without loss of generality, in this paper, we consider the case where clock N acts as the reference clock for all the measurements on clock differences. In particular, the measurement of the overall N-clock ensemble is written as

$$\boldsymbol{y}[k] := \underbrace{\begin{bmatrix} \Delta h^1[k] - \Delta h^N[k] \\ \vdots \\ \Delta h^{m-1}[k] - \Delta h^N[k] \end{bmatrix}}_{(C\otimes\overline{V})\boldsymbol{x}[k]} + \boldsymbol{w}[k] \in \mathbb{R}^{N-1} \tag{6}$$

where

$$\overline{V} := \begin{bmatrix} I_{N-1} & -\mathbb{1}_{N-1} \end{bmatrix} \in \mathbb{R}^{(N-1)\times N}$$

and $\boldsymbol{w} = [w_1, \dots, w_{N-1}]^\mathsf{T} \in \mathbb{R}^{N-1}$ is the measurement noise which is a white Gaussian process such that

$$\mathbb{E}\big[\boldsymbol{w}[k]\big] = 0, \quad \mathbb{E}\big[\boldsymbol{w}[k]\boldsymbol{w}^\mathsf{T}[k]\big] = rI_{N-1} \tag{7}$$

for some positive value $r \in \mathbb{R}_+$.

Then, the discrete-time system model of the overall N-clock ensemble considered in the paper is given as

$$\Sigma : \begin{cases} \boldsymbol{x}[k+1] = (A \otimes I_N)\boldsymbol{x}[k] + \boldsymbol{v}[k] \\ \boldsymbol{y}[k] = (C \otimes \overline{V})\boldsymbol{x}[k] + \boldsymbol{w}[k] \end{cases} \tag{8}$$

where the covariance matrix of the system noise $\boldsymbol{v}[k]$ is defined as

$$\mathbb{Q} := \mathbb{E}\big[\boldsymbol{v}[k]\boldsymbol{v}^\mathsf{T}[k]\big] = Q \otimes I_N$$

for the homogeneous clock ensemble.

C. Mission in Time Scale Generations: Better Prediction

Assuming that the weights of the homogeneous N-clock ensemble, corresponding to the reliability of the individual clocks, are all equal, the ideal and generated clock reading of the N-clock ensemble are given as

$$h_0[k] = \sum\nolimits_{i=1}^m \tfrac{1}{N}(h^j[k] - \Delta h^j[k])$$

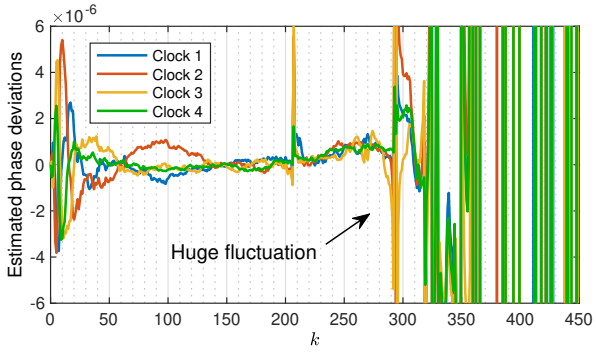

Fig. 1. Example of numerical instability in a 4-clock ensemble.

$$\hat{h}_0[k] = \sum_{i=1}^{m} \tfrac{1}{N}(h^j[k] - \hat{\Delta}h^j[k])$$

respectively, where $h^j[k]$ is the actual clock reading at time t_k, $\Delta h^j[k]$ is the exact time deviation at time t_k, and $\hat{\Delta}h^j[k]$ is its predicted value. Then the accuracy of the generated clock reading is characterized by the *Temps Atomique* [3]

$$\mathrm{TA}[k] := h_0[k] - \hat{h}_0[k] = \tfrac{C}{N}\big(I_n \otimes \mathbb{1}_N^{\mathsf{T}}\big)(\boldsymbol{x}[k] - \hat{\boldsymbol{x}}[k]) \quad (9)$$

where $\hat{\boldsymbol{x}}[k]$ denotes the predicted state. A small difference $\mathrm{TA}[k]$ indicates high accuracy of the generated time scale. Consequently, the main mission in time scale generation is finding a good prediction algorithm that well predicts the internal state $\boldsymbol{x}[k]$ over the discrete-time sequence $\{t_0, t_1, \ldots, t_T\}$.

III. Main Results

In this section, we begin with introducing the problem of the conventional Kalman filter for the homogeneous atomic clock ensemble, and then present the results of spectral decomposition to clarify why numerical instability happens. Specifically, given an initial covariance matrix $\boldsymbol{P}_0$ of the estimation error, the dynamics of the conventional Kalman filter for time-scale generation can be given by

$$\hat{\boldsymbol{x}}[k+1] = (A \otimes I_N)\hat{\boldsymbol{x}}[k] + \boldsymbol{G}_k\Big\{\boldsymbol{y}[k] - (C \otimes \overline{V})\hat{\boldsymbol{x}}[k]\Big\} \quad (10)$$

where $\boldsymbol{G}_k$ is the Kalman gain defined as

$$\boldsymbol{G}_k := \boldsymbol{P}_k(C \otimes \overline{V})^{\mathsf{T}}\big\{(C \otimes \overline{V})\boldsymbol{P}_k(C \otimes \overline{V})^{\mathsf{T}} + rI_{N-1}\big\}^{-1} \quad (11)$$

with the error covariance matrix $\boldsymbol{P}_k$ defined in the discrete-time algebraic Riccati equation (12).

The Kalman filter is an optimal estimator as the discrete-time algebraic Riccati equation (12) may determine the solution of a special infinite-horizon time-invariant Linear-Quadratic Regulator problem minimizing the mean squared error $\mathbb{E}\big[\|\boldsymbol{x}[k] - \hat{\boldsymbol{x}}[k]\|^2\big]$. In such a case, the Kalman gain $\boldsymbol{K}_k$ in the update rules (11) and (12) is the optimal gain in (10). However, in actual implementation, huge fluctuations may occur along with the time that goes (see the example in Fig. 1). This phenomenon is known as numerical instability in [9] for time-scale generation via atomic clock ensembles.

Before we present our main results, we introduce the following lemma as a preliminary.

Lemma 1: Consider a symmetric matrix $A \in \mathbb{R}^{n\times n}$. Let $V_1 \in \mathbb{R}^{n\times m}$ and $V_2 \in \mathbb{R}^{n\times(n-m)}$ satisfying $\mathsf{im}\, V_1 \oplus \mathsf{im}\, V_2 = \mathbb{R}^n$, $AV_1 = V_1A_1$, and $AV_2 = V_2A_2$ for some $A_1 \in \mathbb{R}^{m\times m}$ and $A_2 \in \mathbb{R}^{(n-m)\times(n-m)}$. Then,

$$A = V_1A_1V_1^{\dagger} + V_2A_2V_2^{\dagger}.$$

Furthermore,

$$A_1 = V_1^{\dagger}AV_1, \quad A_2 = V_2^{\dagger}AV_2$$

have the spectra such that

$$\lambda(A) = \lambda(A_1) \cup \lambda(A_2).$$

Proof: The proof is omitted. ∎

A. Essential Reason

To theoretically understand the essential reason why numerical instability happens, we apply spectral decomposition to the task of time generation in the following results.

Theorem 1: Consider an N-clock ensemble with the conventional Kalman filter algorithms (10)–(12). If the initial error covariance matrix $\boldsymbol{P}_0$ satisfies

$$\boldsymbol{P}_0(I_n \otimes \mathbb{1}_N) = (I_n \otimes \mathbb{1}_N)\hat{P}_0 \quad (13)$$

$$\boldsymbol{P}_0(I_n \otimes \overline{V})^{\dagger} = (I_n \otimes \overline{V})^{\dagger}\check{P}_0 \quad (14)$$

for some matrices $\hat{P}_0$ and $\check{P}_0$, then the error covariance matrix $\boldsymbol{P}_k$ in the CKF algorithms can be decomposed as

$$\boldsymbol{P}_k = (I_n \otimes \mathbb{1}_N)\hat{P}_k(I_n \otimes \mathbb{1}_N)^{\dagger} + (I_n \otimes \overline{V})^{\dagger}\check{P}_k(I_n \otimes \overline{V}) \quad (15)$$

with the matrices $\hat{P}_k$ and $\check{P}_k$ such that

$$\hat{P}_{k+1} = A\hat{P}_kA^{\mathsf{T}} + Q \quad (16)$$

$$\begin{aligned}\check{P}_{k+1} =& -(A \otimes I_{N-1})\check{\boldsymbol{G}}_k(C \otimes I_{N-1})\check{P}_k(A \otimes I_{N-1})^{\mathsf{T}} \\ &+ (A \otimes I_{N-1})\check{P}_k(A \otimes I_{N-1})^{\mathsf{T}} + Q \otimes I_{N-1}\end{aligned} \quad (17)$$

where $\check{\boldsymbol{G}}_k$ is given in (18).

Proof: Note from the fact $\mathbb{1}_N^{\mathsf{T}}\overline{V}^{\dagger} = 0$ that the condition $\mathsf{im}\,\mathbb{1}_N \oplus \mathsf{im}\,\overline{V}^{\dagger} = \mathbb{R}^{nN}$ is satisfied and thus it follows from Lemma 1 that (15) holds for the initial $\boldsymbol{P}_0$. The condition (13) indicates that

$$\begin{aligned}\boldsymbol{P}_{k+1}(I_n \otimes \mathbb{1}_N) =& (A \otimes I_N)\boldsymbol{P}_k(I_n \otimes \mathbb{1}_N)A^{\mathsf{T}} + (I_n \otimes \mathbb{1}_N)Q \\ &- (A \otimes I_N)\boldsymbol{G}_k(C \otimes \overline{V})\boldsymbol{P}_k(I_n \otimes \mathbb{1}_N)A^{\mathsf{T}} \\ =& (A \otimes I_N)(I_n \otimes \mathbb{1}_N)\hat{P}_kA^{\mathsf{T}} + (I_n \otimes \mathbb{1}_N)Q \\ &- (A \otimes I_N)\boldsymbol{G}_k\underbrace{(C \otimes \overline{V})(I_n \otimes \mathbb{1}_N)}_{=0}\hat{P}_kA^{\mathsf{T}} \\ =& (I_n \otimes \mathbb{1}_N)\hat{P}_{k+1}\end{aligned} \quad (19)$$

holds for any $k \in \{0, 1, 2, \ldots\}$.

In terms of the matrix $\check{P}_k$, because of

$$(A \otimes I_N)(I_n \otimes \overline{V})^{\dagger} = (I_n \otimes \overline{V})^{\dagger}(A \otimes I_{N-1}), \quad (20)$$

the condition (14) indicates that (21) holds for any $k = 0, 1, 2, \ldots$. Thus, the proof is complete by Lemma 1. ∎

Remark 1: In numerical implementation, the calculations of high dimensional matrices in the Kalman filtering algorithms are costly and difficult. However, the result of

$$\boldsymbol{P}_{k+1} = (A\otimes I_N)\Big[\boldsymbol{P}_k - \underbrace{\boldsymbol{P}_k(C\otimes\overline{V})^{\mathsf{T}}\big((C\otimes\overline{V})\boldsymbol{P}_k(C\otimes\overline{V})^{\mathsf{T}}+rI_{N-1}\big)^{-1}}_{\boldsymbol{G}_k}(C\otimes\overline{V})\boldsymbol{P}_k\Big](A\otimes I_N)^{\mathsf{T}}+\mathbb{Q} \tag{12}$$

$$\check{\boldsymbol{G}}_k = \check{P}_k(C\otimes I_{N-1})^{\mathsf{T}}\big\{(C\otimes I_{N-1})\check{P}_k(C\otimes I_{N-1})^{\mathsf{T}}+r(\overline{V}\overline{V}^{\mathsf{T}})^{-1}\big\}^{-1} \tag{18}$$

$$\begin{aligned}\boldsymbol{P}_{k+1}(I_n\otimes\overline{V})^{\dagger} =& (I_n\otimes\overline{V})^{\dagger}(A\otimes I_{N-1})\check{P}_k(A\otimes I_{N-1})^{\mathsf{T}}+(I_n\otimes\overline{V})^{\dagger}(Q\otimes I_{N-1})\\ &-(I_n\otimes\overline{V})^{\dagger}(A\otimes I_{N-1})\underbrace{\check{P}_k(C^{\mathsf{T}}\otimes\overline{V}\overline{V}^{\mathsf{T}})\Big\{(C\otimes\overline{V})\boldsymbol{P}_k(C\otimes\overline{V})^{\mathsf{T}}+rI_{N-1}\Big\}^{-1}}_{=\check{P}_k(C\otimes I_{N-1})^{\mathsf{T}}\left\{(C\otimes I_{N-1})\check{P}_k(C\otimes I_{N-1})^{\mathsf{T}}+r(\overline{V}\overline{V}^{\mathsf{T}})^{-1}\right\}^{-1}=\check{\boldsymbol{G}}_k}(C\otimes\overline{V}\overline{V}^{\dagger})\check{P}_k(A\otimes I_{N-1})^{\mathsf{T}}\\ =&(I_n\otimes\overline{V})^{\dagger}\Big\{(A\otimes I_{N-1})\Big[\check{P}_k-\check{\boldsymbol{G}}_k(C\otimes I_{N-1})\check{P}_k\Big](A\otimes I_{N-1})^{\mathsf{T}}+(Q\otimes I_{N-1})\Big\}=(I_n\otimes\overline{V})^{\dagger}\check{P}_{k+1}\end{aligned} \tag{21}$$

Theorem 1 indicates that the conventional Kalman filtering algorithm in (10)–(12) can be equivalently reconstructed as (10) and (11) with (15)–(18) where calculation time are supposed to be shortened since the dimension of the calculated matrix is reduced from nN to $nN-n$.

Remark 2: Note that the equation (17) along with (18) can be understood as a discrete-time algebraic Riccati equation which converges to a steady-state value since the pair (A,C) is observable. Thus, the essence of Theorem 1 is that the error covariance matrix $\boldsymbol{P}_k$ of the Kalman filter can be decomposed into a diverging part $\hat{P}_k$ and a converging part $\check{P}_k$ (see Fig. 2). Moreover, because

$$\begin{aligned}&\boldsymbol{P}_k(C\otimes\overline{V})^{\mathsf{T}} = \boldsymbol{P}_k(I_n\otimes\overline{V})^{\dagger}(C\otimes\overline{V}\overline{V}^{\mathsf{T}})\\ &=(I_n\otimes\overline{V})^{\dagger}\check{P}_k(C\otimes\overline{V}\overline{V}^{\mathsf{T}})\end{aligned} \tag{22}$$

$$\begin{aligned}&(C\otimes\overline{V})\boldsymbol{P}_k(C\otimes\overline{V})^{\mathsf{T}}\\ &=(C\otimes I_{N-1})(I_n\otimes\overline{V})\boldsymbol{P}_k(I_n\otimes\overline{V})^{\dagger}(C\otimes\overline{V}\overline{V}^{\mathsf{T}})\\ &=(C\otimes I_{N-1})\check{P}_k(C\otimes\overline{V}\overline{V}^{\mathsf{T}})\end{aligned} \tag{23}$$

the Kalman gain $\boldsymbol{G}_k$ of the Kalman filter in (11) is solely influenced by the converging part $\check{P}_k$ instead of the diverging part $\hat{P}_k$, i.e, $\boldsymbol{G}_k$ converges to a steady-state value if there is no computation error. However, because there must be a computation error in practical implementation, $(C\otimes\overline{V})\boldsymbol{P}_k(C\otimes\overline{V})^{\mathsf{T}}$ may be no longer equal to (23) and hence numerical instability occurs.

B. Further Decomposition to Reduce Computation Costs

The following result indicates that the decomposed error covariance matrix $\check{P}_k$ of (17) can be further decomposed to obtain a new expression with some lower-dimensional matrices. The calculation cost can be further saved from the reduced algorithms (10), (11) with (15)–(18).

Theorem 2: Consider an N-clock ensemble with the CKF algorithms (10)–(12). If the initial error covariance matrix $\boldsymbol{P}_0$ satisfies $\boldsymbol{P}_0 = pI_{nN}$ for some non-negative scalar $p\geq 0$, then the error covariance matrix $\boldsymbol{P}_k$ of the CKF algorithms

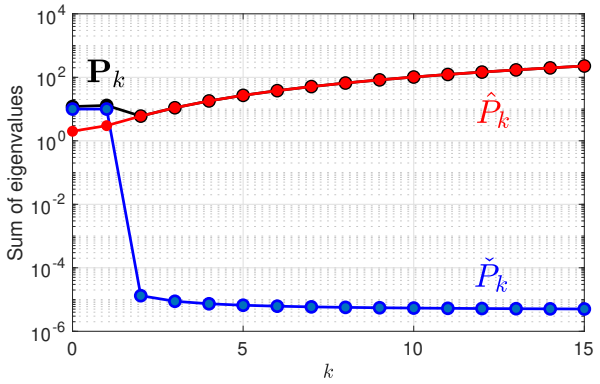

Fig. 2. Trace values of the error covariance matrix $\boldsymbol{P}_k$, the decomposed divergent part $\hat{P}_k$, and the converging part $\check{P}_k$.

can decomposed as

$$\begin{aligned}\boldsymbol{P}_k =& \tfrac{1}{N(N-1)}\left(I_n\otimes\begin{bmatrix}\mathbb{1}_{N-1}\\ -(N-1)\end{bmatrix}\right)\check{X}_k\left(I_n\otimes\begin{bmatrix}\mathbb{1}_{N-1}\\ -(N-1)\end{bmatrix}\right)^{\mathsf{T}}\\ &+\check{Y}_k\otimes\begin{bmatrix}I_{N-1}-\frac{1}{N-1}\mathbb{1}_{N-1}\mathbb{1}_{N-1}^{\mathsf{T}} & 0\\ 0 & 0\end{bmatrix}\\ &+\tfrac{1}{N}(I_n\otimes\mathbb{1}_N)\hat{P}_k(I_n\otimes\mathbb{1}_N)^{\mathsf{T}}\end{aligned} \tag{24}$$

where the matrix $\hat{P}_k$ follows the dynamics (16), and the matrices $\check{X}_k$ and $\check{Y}_k$ follows

$$\begin{cases}\hat{P}_{k+1} = A\hat{P}_kA^{\mathsf{T}}+Q\\ \check{X}_{k+1} = A\check{X}_kA^{\mathsf{T}}+Q-A\check{X}_kC^{\mathsf{T}}(C\check{X}_kC^{\mathsf{T}}+\frac{r}{N})^{-1}C\check{X}_kA^{\mathsf{T}}\\ \check{Y}_{k+1} = A\check{Y}_kA^{\mathsf{T}}+Q-A\check{Y}_kC^{\mathsf{T}}(C\check{Y}_kC^{\mathsf{T}}+r)^{-1}C\check{Y}_kA^{\mathsf{T}}\end{cases} \tag{25}$$

with $\hat{P}_0=\check{X}_0=\check{Y}_0=pI_n$ for any $k=0,1,2,\ldots$.

Proof: First of all, the condition $\boldsymbol{P}_0=pI_{nN}$ indicates that the conditions (13) and (14) in Theorem 1 are satisfied with $\hat{P}_0=pI_n$ and $\check{P}_0=pI_{n(N-1)}$. Therefore, it follows from Theorem 1 that the error covariance matrix $\boldsymbol{P}_k$ of the CKF algorithms can be decomposed as (15) with $\hat{P}_k$ following (16) and $\check{P}_k$ following (17) and (18). Now, note that

$$\overline{w} := \begin{bmatrix}I_{N-2}\\ -\mathbb{1}_{N-2}^{\mathsf{T}}\end{bmatrix}\in\mathbb{R}^{(N-1)\times(N-2)} \tag{26}$$

satisfies $\mathbb{1}_{N-1}^{\mathsf{T}}\overline{w}=0$ and $\mathsf{im}\,\mathbb{1}_{N-1}\oplus\mathsf{im}\,\overline{w}=\mathbb{R}^{N-1}$ holds. Moreover, note that

$$\check{P}_0(I_n\otimes\mathbb{1}_{N-1})=(I_n\otimes\mathbb{1}_{N-1})\check{X}_0 \tag{27}$$
$$\check{P}_0(I_n\otimes\overline{w})=(I_n\otimes\overline{w})\check{Z}_0 \tag{28}$$

with $\check{Z}_0=\check{Y}_0\otimes I_{N-2}$ due to the facts $\check{P}_0=pI_{n(N-1)}$ and $\hat{P}_0=\check{X}_0=\check{Y}_0=pI_n$. Letting λ and Λ satisfy

$$\{(C\otimes I_{N-1})\check{P}_k(C\otimes I_{N-1})^{\mathsf{T}}+r(\overline{V}\overline{V}^{\mathsf{T}})^{-1}\}^{-1}\mathbb{1}_{N-1}=\lambda\mathbb{1}_{N-1}$$
$$\{(C\otimes I_{N-1})\check{P}_k(C\otimes I_{N-1})^{\mathsf{T}}+r(\overline{V}\overline{V}^{\mathsf{T}})^{-1}\}^{-1}\overline{w}=\overline{w}\Lambda,$$

it follows from

$$\begin{aligned}\mathbb{1}_{N-1}=&\lambda\big\{(C\otimes I_{N-1})\check{P}_k(C\otimes I_{N-1})^{\mathsf{T}}+r(\overline{V}\overline{V}^{\mathsf{T}})^{-1}\big\}\mathbb{1}_{N-1}\\ =&\lambda\big\{(C\otimes I_{N-1})\check{P}_k(I_n\otimes\mathbb{1}_{N-1})C^{\mathsf{T}}+r(\overline{V}\overline{V}^{\mathsf{T}})^{-1}\mathbb{1}_{N-1}\big\}\\ =&\lambda\big\{(C\otimes\mathbb{1}_{N-1})\check{X}_kC^{\mathsf{T}}+r\tfrac{1}{N}\mathbb{1}_{N-1}\big\}\\ =&\lambda\mathbb{1}_{N-1}\big\{C\check{X}_kC^{\mathsf{T}}+\tfrac{r}{N}\big\}\end{aligned} \tag{29}$$

and

$$\begin{aligned}\overline{w}=&\big\{(C\otimes I_{N-1})\check{P}_k(C\otimes I_{N-1})^{\mathsf{T}}+r(\overline{V}\overline{V}^{\mathsf{T}})^{-1}\big\}\overline{w}\Lambda\\ =&\big\{(C\otimes I_{N-1})\check{P}_k(I_n\otimes\overline{w})(C\otimes I_{N-2})^{\mathsf{T}}+r(\overline{V}\overline{V}^{\mathsf{T}})^{-1}\overline{w}\big\}\Lambda\\ =&\big\{(C\otimes\overline{w})\check{Z}_k(C\otimes I_{N-2})^{\mathsf{T}}+r\overline{w}\big\}\Lambda\\ =&\overline{w}\big\{(C\otimes I_{N-2})\check{Z}_k(C\otimes I_{N-2})^{\mathsf{T}}+rI_{N-2}\big\}\Lambda\end{aligned} \tag{30}$$

that the expressions of λ and Λ are given by

$$\lambda=\big\{C\check{X}_kC^{\mathsf{T}}+\tfrac{r}{N}\big\}^{-1} \tag{31}$$
$$\Lambda=\big\{(C\otimes I_{N-2})\check{Z}_k(C\otimes I_{N-2})^{\mathsf{T}}+rI_{N-2}\big\}^{-1}. \tag{32}$$

Thus, it follows from (27) that (33) holds $k=0,1,2,\ldots$.

In terms of the matrix $\check{Z}_k$, it follows from (28) that (34) holds $k=0,1,2,\ldots$, where $\check{Z}_{k+1}$ follows

$$\begin{aligned}\check{Z}_{k+1}=&(A\otimes I_{N-2})\check{Z}_k(A\otimes I_{N-2})^{\mathsf{T}}+Q\otimes I_{N-2}\\ &-(A\otimes I_{N-2})\check{Z}_k(C\otimes I_{N-2})^{\mathsf{T}}\\ &\cdot\big\{(C\otimes I_{N-2})\check{Z}_k(C\otimes I_{N-2})^{\mathsf{T}}+rI_{N-2}\big\}^{-1}\\ &\cdot(C\otimes I_{N-2})\check{Z}_k(A\otimes I_{N-2})^{\mathsf{T}}\end{aligned} \tag{35}$$

for $k=0,1,2,\ldots$. Here, the condition $\check{Z}_0=\check{Y}_0\otimes I_{N-2}$ indicates that

$$\check{Z}_k=\check{Y}_k\otimes I_{N-2},\quad k=0,1,2,\ldots.$$

Thus, it follows from Lemma 1 that the decomposed matrix $\check{P}_k$ can be further decomposed as

$$\begin{aligned}\check{P}_k=&(I_n\otimes\mathbb{1}_{N-1})\hat{X}_k(I_n\otimes\mathbb{1}_{N-1})^{\dagger}\\ &+(I_n\otimes\overline{w})(\check{Y}_k\otimes I_{N-2})(I_n\otimes\overline{w})^{\dagger}\\ =&(I_n\otimes\mathbb{1}_{N-1})\hat{X}_k(I_n\otimes\mathbb{1}_{N-1})^{\dagger}+\check{Y}_k\otimes\overline{w}\overline{w}^{\dagger}\end{aligned} \tag{36}$$

Now, substituting (36) to (15), we have

$$\begin{aligned}\boldsymbol{P}_k=&(I_n\otimes\overline{V})^{\dagger}\check{P}_k(I_n\otimes\overline{V})+(I_n\otimes\mathbb{1}_N)\hat{P}_k(I_n\otimes\mathbb{1}_N)^{\dagger}\\ =&(I_n\otimes\overline{V}^{\dagger}\mathbb{1}_{N-1})\hat{X}_k(I_n\otimes\overline{V}^{\dagger}\mathbb{1}_{N-1})^{\dagger}\\ &+\check{Y}_k\otimes\overline{V}^{\dagger}\overline{w}\overline{w}^{\dagger}\overline{V}+\tfrac{1}{N}(I_n\otimes\mathbb{1}_N)\hat{P}_k(I_n\otimes\mathbb{1}_N)^{\mathsf{T}}\\ =&\tfrac{1}{N(N-1)}\left(I_n\otimes\begin{bmatrix}\mathbb{1}_{N-1}\\-(N-1)\end{bmatrix}\right)\hat{X}_k\left(I_n\otimes\begin{bmatrix}\mathbb{1}_{N-1}\\-(N-1)\end{bmatrix}\right)^{\mathsf{T}}\\ &+\check{Y}_k\otimes\begin{bmatrix}\overline{w}\overline{w}^{\dagger}&0\\0&0\end{bmatrix}+\tfrac{1}{N}(I_n\otimes\mathbb{1}_N)\hat{P}_k(I_n\otimes\mathbb{1}_N)^{\mathsf{T}}.\end{aligned}$$

which is same as (24) due to

$$\overline{w}\overline{w}^{\dagger}=I_{N-1}-\tfrac{1}{N-1}\mathbb{1}_{N-1}\mathbb{1}_{N-1}^{\mathsf{T}}.$$

The proof is completed. ■

IV. Numerical Simulations

In this section, we provide an application example to demonstrate our results. Specifically, consider a homogeneous third-order atomic clock ensemble with $N=3$ clocks. The coefficients of the model are set to the standard values of $q_1^2=9e-26$, $q_2^2=7.5e-34$, and $q_3^2=1e-47$. The sampling interval is set to $\tau=1$. The variance of the measurement noise is set to $r=1e-12$. In the simulation, both of the initial state $\boldsymbol{x}[0]$ of this 3-clock ensemble and the initial predicted value $\hat{\boldsymbol{x}}[0]$ are set to $1e-28\mathbb{1}_9$. The time scale difference $\mathrm{TA}[k]$ of a single stochastic path for $\boldsymbol{P}_0=1e{-}13I, 4e{-}13I, 8e{-}13I$ are shown in Fig. 3, which reveals the fact that the performance of the Kalman filter with and without covariance reduction significantly depends on the initial covariance $\boldsymbol{P}_0$. In addition, Fig. 3 is able to reveal the fact that the short-term performances of the naive Kalman filter and Kalman filters with Brown's and Greenhall's correction methods are good, but the performances turn to bad in a long term. However, our new approach shows good performances in both short-term and long-term evaluations compared to those existing methods.

V. Conclusion

We studied the prediction problem for the atomic clock ensembles to generate an accurate time scale. To clarify the essential reason why numerical instability happens in the Kalman filter for homogeneous atomic clock ensembles, we applied spectral decomposition to the task of time generation. In particular, we showed that the error covariance matrix of the Kalman filter can be decomposed as a diverging part and a converging part where the Kalman gain is solely influenced by the converging part instead of the diverging part. We presented several alternative methods to the conventional Kalman filter to reduce computation cost where the covariance of Kalman filter can be computed rigorously only using three n-dimensional Riccati iterations instead of an nN-dimensional Riccati iterations for an n-order clock model with N clocks.

$$
\begin{aligned}
\check{P}_{k+1}(I_n \otimes \mathbb{1}_{N-1}) =& (A \otimes I_{N-1})\check{P}_k(I_n \otimes \mathbb{1}_{N-1})A^{\mathsf{T}} + (I_n \otimes \mathbb{1}_{N-1})Q - (A \otimes I_{N-1})\check{\boldsymbol{G}}_k(C \otimes I_{N-1})\check{P}_k(I_n \otimes \mathbb{1}_{N-1})A^{\mathsf{T}} \\
=& (I_n \otimes \mathbb{1}_{N-1})A\check{X}_k A^{\mathsf{T}} + (I_n \otimes \mathbb{1}_{N-1})Q - (A \otimes I_{N-1})\check{\boldsymbol{G}}_k \mathbb{1}_{N-1} C\check{X}_k A^{\mathsf{T}} \\
=& (I_n \otimes \mathbb{1}_{N-1})A\check{X}_k A^{\mathsf{T}} + (I_n \otimes \mathbb{1}_{N-1})Q - \lambda(A \otimes I_{N-1})\check{P}_k \underbrace{(C \otimes I_{N-1})^{\mathsf{T}}\mathbb{1}_{N-1}}_{=(I_n \otimes \mathbb{1}_{N-1})C^{\mathsf{T}}} C\check{X}_k A^{\mathsf{T}} \\
=& (I_n \otimes \mathbb{1}_{N-1})\Big\{A\check{X}_k A^{\mathsf{T}} + Q - \lambda A\check{X}_k C^{\mathsf{T}} C\check{X}_k A^{\mathsf{T}}\Big\} = (I_n \otimes \mathbb{1}_{N-1})\check{X}_{k+1}
\end{aligned} \tag{33}
$$

$$
\begin{aligned}
\check{P}_{k+1}(I_n \otimes \overline{w}) =& (A \otimes I_{N-1})\check{P}_k(I_n \otimes \overline{w})(A \otimes I_{N-2})^{\mathsf{T}} + (I_n \otimes \overline{w})(Q \otimes I_{N-2}) \\
& - (A \otimes I_{N-1})\check{\boldsymbol{G}}_k(C \otimes I_{N-1})\check{P}_k(I_n \otimes \overline{w})(A \otimes I_{N-2})^{\mathsf{T}} \\
=& (I_n \otimes \overline{w})(A \otimes I_{N-2})\check{Z}_k(A \otimes I_{N-2})^{\mathsf{T}} + (I_n \otimes \overline{w})(Q \otimes I_{N-2}) \\
& - (A \otimes I_{N-1})\check{\boldsymbol{G}}_k \overline{w}(C \otimes I_{N-2})\check{Z}_k(A \otimes I_{N-2})^{\mathsf{T}} \\
=& (I_n \otimes \overline{w})(A \otimes I_{N-2})\check{Z}_k(A \otimes I_{N-2})^{\mathsf{T}} + (I_n \otimes \overline{w})(Q \otimes I_{N-2}) \\
& - (A \otimes I_{N-1})\check{P}_k(C \otimes I_{N-1})^{\mathsf{T}}\overline{w}\Lambda(C \otimes I_{N-2})\check{Z}_k(A \otimes I_{N-2})^{\mathsf{T}} \\
=& (I_n \otimes \overline{w})(A \otimes I_{N-2})\check{Z}_k(A \otimes I_{N-2})^{\mathsf{T}} + (I_n \otimes \overline{w})(Q \otimes I_{N-2}) \\
& - (A \otimes I_{N-1})\check{P}_k(I_n \otimes \overline{w})(C \otimes I_{N-2})^{\mathsf{T}}\Lambda(C \otimes I_{N-2})\check{Z}_k(A \otimes I_{N-2})^{\mathsf{T}} \\
=& (I_n \otimes \overline{w})\Big\{(A \otimes I_{N-2})\check{Z}_k(A \otimes I_{N-2})^{\mathsf{T}} + Q \otimes I_{N-2} \\
& \qquad - (A \otimes I_{N-2})\check{Z}_k(C \otimes I_{N-2})^{\mathsf{T}}\Lambda(C \otimes I_{N-2})\check{Z}_k(A \otimes I_{N-2})^{\mathsf{T}}\Big\} = (I_n \otimes \overline{w})\check{Z}_{k+1}
\end{aligned} \tag{34}
$$

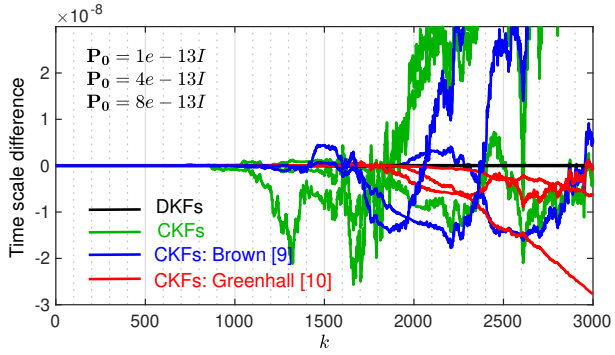

Fig. 3. Time scale difference TA$[k]$ under the conventional Kalman filter (CKF), Kalman filter with Brown and Greenhall's correction, and our decomposed approach (DKF) for different initial covariance matrices.

ACKNOWLEDGMENTS

This paper includes the results of research and development conducted by the Ministry of Internal Affairs and Communications (MIC) under its "Research and Development for Expansion of Radio Resources (JPJ000254)" program.

REFERENCES

[1] Y. Wu, X. Zhu, Y. Huang, G. Sun, and G. Ou, "Uncertainty derivation and performance analyses of clock prediction based on mathematical model method," *IEEE Transactions on Instrumentation and Measurement*, vol. 64, no. 10, pp. 2792–2801, 2015.

[2] L. Galleani and P. Tavella, "On the use of the kalman filter in timescales," *Metrologia*, vol. 40, no. 3, p. S326, 2003.

[3] ——, "Time and the kalman filter," *IEEE Control Systems Magazine*, vol. 30, no. 2, pp. 44–65, 2010.

[4] C. A. Greenhall, "A review of reduced kalman filters for clock ensembles," *IEEE Transactions on Ultrasonics, Ferroelectrics, and Frequency Control*, vol. 59, no. 3, pp. 491–496, 2012.

[5] C. Trainotti, G. Giorgi, and C. Günther, "Detection and identification of faults in clock ensembles with the generalized likelihood ratio test," *Metrologia*, vol. 59, no. 4, p. 045010, 2022.

[6] C. De Souza, M. Gevers, and G. Goodwin, "Riccati equations in optimal filtering of nonstabilizable systems having singular state transition matrices," *IEEE Transactions on Automatic control*, vol. 31, no. 9, pp. 831–838, 1986.

[7] F. Auger, M. Hilairet, J. M. Guerrero, E. Monmasson, T. Orlowska-Kowalska, and S. Katsura, "Industrial applications of the kalman filter: A review," *IEEE Transactions on Industrial Electronics*, vol. 60, no. 12, pp. 5458–5471, 2013.

[8] M. Gödel, T. D. Schmidt, and J. Furthner, "Kalman filter approaches for a mixed clock ensemble," in *2017 Joint Conference of the European Frequency and Time Forum and IEEE International Frequency Control Symposium (EFTF/IFCS)*. IEEE, 2017, pp. 666–672.

[9] K. R. Brown, *The theory of the GPS composite clock*. Institute of Navigation, 1991.

[10] C. A. Greenhall, "A kalman filter clock ensemble algorithm that admits measurement noise," *Metrologia*, vol. 43, no. 4, p. S311, 2006.

[11] Y. Yan, T. Kawaguchi, Y. Yano, Y. Hanado, and T. Ishizaki, "Structured kalman filter for time scale generation in atomic clock ensembles," *arXiv preprint arXiv:2305.05894*, 2023.

[12] Y. Yan, N. J. Jensen, T. Kawaguchi, Y. Yano, Y. Hanado, and T. Ishizaki, "Possibility of prediction improvements for atomic clock ensembles: Basis selection in undetectable systems," in *Proceedings of The 22nd IFAC World Congress*, 2023, pp. 6500–6505.

[13] Y. Yan, T. Kawaguchi, Y. Yano, Y. Hanado, and T. Ishizaki, "Relations between generalized jst algorithm and kalman filtering algorithm for time scale generation," *arXiv preprint arXiv:2308.12548*, 2023.